Platycarya strobilacea leaf extract protects mice brain with focal cerebral ischemia by antioxidative property

Ji Hye Lee[1], Ji Heun Jeong[1], Young-Gil Jeong[1], Do-Kyung Kim[1], Nam-Seob Lee[1], Chun Soo Na[2], Eun Soo Doh[3], Seung Yun Han[1]

[1]Department of Anatomy, Konyang University College of Medicine, Daejeon, [2]Lifetree Co., Ltd., Suwon, [3]Department of Herbal Health and Pharmacy, Joongbu University College of Health and Welfare, Geumsan, Korea

Abstract: The leaf extract of *Platycarya strobilacea* (PSL) has long been recognized as possessing various health-promoting activities. However, information on its possible protective effects against ischemic stroke is currently lacking. Here, using a mouse model of focal cerebral ischemia (fCI), we studied the protective potential of an oral supplement of PSL. Mice were randomly divided into four groups: SO, a group subjected to a sham-operation; VEH, pretreated with distilled water and subjected to middle cerebral artery occlusion and reperfusion (MCAO/R); PSL-L and PSL-H, pretreated with low (20 mg/kg) and high (100 mg/kg) doses of PSL, respectively, and subjected to the MCAO/R procedure. PSL was administered via an oral route daily for 8 days prior to surgery. We then measured the infarct volumes and sensorimotor deficits and studied the underlying antioxidant mechanisms by quantifying apoptosis, reactive oxygen species (ROS) generation, oxidative damages, and antioxidant enzymes in the ischemic cortex. The results showed a marked attenuation in infarct volume and sensorimotor deficits in both the PSL-L and PSL-H groups when compared with VEH. The terminal deoxynucleotidyl transferase dUTP nick end labeling and the immunohistochemical detection of the cleaved caspase-3 revealed that PSL could reduce cellular apoptosis in the ischemic lesion in a dose-dependent manner. The dihydroethidium-fluorescence, 4-hydroxynonenal, and 8-hydroxyl-2'-deoxyguanosine immunoreactivities in the ischemic lesion were markedly attenuated in the PSL-L group compared with the VEH group, indicating that PSL could attenuate ROS generation and the associated oxidative damage in the ischemic cortex. Finally, western blot results indicated that PSL can upregulate levels of heme oxygenase-1 (HO-1), an antioxidant enzyme, in the lesion area. Together, these results suggest that PSL can exert protective effects against fCI, and the mechanism may involve HO-1 upregulation.

Key words: *Platycarya strobilacea* leaf, Focal cerebral ischemia, Reactive oxygen species, Antioxidant, Heme oxygenase-1

Received June 25, 2019; Revised July 24, 2019; Accepted September 16, 2019

Corresponding authors:
Seung Yun Han 🆔
Department of Anatomy, Konyang University College of Medicine, 158 Gwanjeodong-ro, Seo-gu, Daejeon 35365, Korea
Tel: +82-42-600-8616, Fax: +82-42-600-8629, E-mail: jjzzy@konyang.ac.kr
Eun Soo Doh 🆔
Department of Herbal Health and Pharmacy, Joongbu University College of Health and Welfare, 201 Chubu-myeon, Daehak-ro, Geumsan 32713, Korea
Tel: +82-41-750-6722, Fax: +82-41-750-6174, E-mail: esdoh@joongbu.ac.kr

*These two authors equally contributed to this work.

Introduction

Focal cerebral ischemia (fCI) is one of the leading causes of death and permanent disability worldwide, resulting in irreversible neuronal damage and loss of sensorimotor function [1, 2]. The only clinically available drug directed at fCI is intravenous administration of recombinant tissue plasminogen activator (rT-PA), a thrombolytic agent [3]. When delivered up to 3.5 hours after the initial insult, rT-PA can attenuate fCI-induced brain damage. However, a majority of patients are not admitted to the clinic within this "golden window" after the onset of fCI; thus, treatment with rT-PA often has decreased efficacy [4]. To overcome this, a thousand pharmaceutical candidates have been screened and suggested as the alternatives to rT-PA. However, almost all the trials have been unsuccessful [5-7]. The resulting pessimism has turned researchers' attention towards the development of a "preventive agent" in an effort to minimize the neuronal damage during a future fCI insult [8-10].

Among the preventive candidates, phytochemicals originating from plants are currently attracting substantial attention. Recent studies have revealed that various polyphenols enriched in plants have various health-promoting effects [11-13]. They are known to possess significant antioxidant capacity, which is considered the main mechanism of conferring the health benefits [14-17]. Since an imbalance between the generation and the clearance of reactive oxygen species (ROS) is known to be the key event in fCI pathogenesis, it is logical that antioxidant capacity of plant polyphenols may confer protection against fCI [18].

Based on the above assumption, this study tested the protective effects of *Platycarya strobilacea* (PS) leaf extract (PSL) on fCI pathogenesis. PS is a small deciduous broad-leaf tree belonging to the wild walnut family and is abundant in Asian countries, including Korea [19, 20]. In traditional medicine, PSL has long been used empirically without scientific rationale. To date, unfortunately, information about the possible efficacies of PSL on specific disease models is rare, except in cases citing its antifungal [21] and anticancer [22] activities. However, recent studies reporting potent antioxidative effects of juglone (5-hydroxy-2-methoxy-1,4-naphthoquinone) [23] and ellagic acid [24], the two key polyphenolic constituents of PSL, suggest that the crude form of PSL may exert a neuroprotective effect. However, there have been no studies elucidating the neuroprotective role of PSL against fCI.

Therefore, this study was designed to investigate the thera-peutic effect and the possible underlying mechanism of PSL against fCI pathogenesis. The *in vivo* therapeutic effect of PSL was examined by measuring infarct volume and the severity of motor deficits, and the antioxidant mechanisms were assessed using oxidative damage-associated apoptosis assays.

Materials and Methods

Preparation of PSL extract

PSL extract was kindly supplied by Lifetree Biotech Co., Ltd. (Suwon, Korea). For the preparation, the leaves of the PS were harvested at Wonju, Gangwon-do, South Korea. The harvested leaves were mixed with water (1:10, w/v), and then eluted with boiling water for 3 hours. The extract was concentrated to a 15 % solid content yield using a vacuum evaporator. The concentrated extract was diluted with an equal volume of dextrin, and freeze-dried in a lyophilizer system (Advantage 2.0, SP Scientific, Warminster, PA, USA). The yield was approximately 4%.

Animals and experimental design

The animal protocol used in this study was reviewed and approved on the basis of the ethical procedures and scientific care by the Institutional Animal Care and Use Committee (IACUC) in Konyang University (Daejeon, Korea). All experimental procedures were performed in accordance with the National Institutes of Health (NIH, Bethesda, MD, USA) Guidelines for the Care and Use of Laboratory Animals, eighth edition [25]. Forty-eight male C57/BL6 mice (25–30 g; 8 weeks) were purchased from Samtako (Osan, Korea). On arrival, the mice were stabilized for 7 days, with access to water and food *ad libitum* at a constant temperature (22°C±2°C) and humidity (40%–60%) with a 12-hour light/dark cycle. Following this, the mice were randomly divided into four groups as follows (n=12 per group): SO, subjected to a sham-operation; VEH, treated with distilled water as a vehicle and a subsequent operation; PSL-L, treated with low dose (20 mg/kg) of PSL and subjected to an operation; and PSL-H, treated with high dose (100 mg/kg) of PSL and subjected to an operation. The operation technique involved 60 minutes of middle cerebral artery occlusion and reperfusion (MCAO/R). Either vehicle or PSL was administered daily by an intraoral route for 8 days prior to MCAO/R. The operated mice were returned to their home cage and kept until sacrifice. The experimental plan is schematically illustrated in Fig. 1.
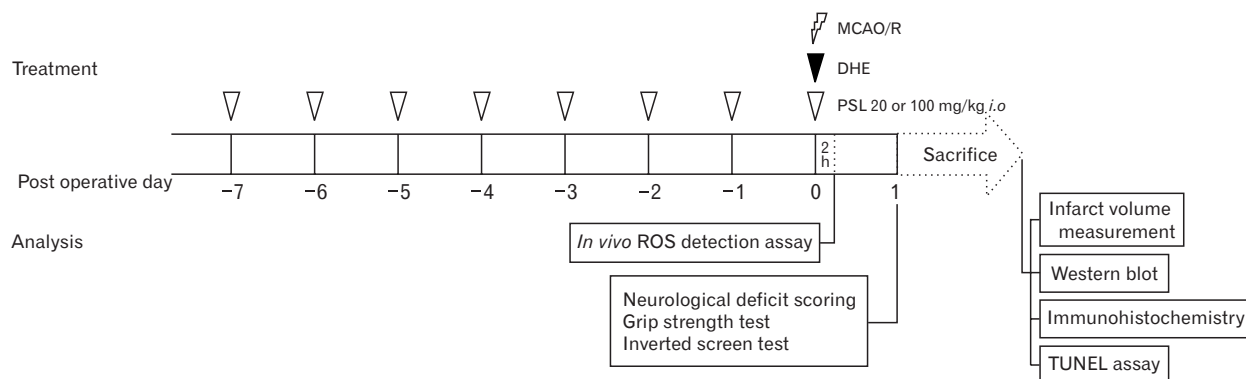
Fig. 1. The experimental protocols used in this study. For the VEH, PSL-L, and PSL-H group, vehicle, 20, or 100 mg/kg of PSL were administered daily via an intraoral route 8 times prior to MCAO/R, respectively. For the SO group, a sham-operation was executed instead of the MCAO/R. For *in vivo* ROS detection, the mice (n=2 per each group) were injected with 10 mg/kg of DHE intravenously just before MCAO/R and sacrificed at 2-hour post-operation for brain sampling. At 24 hours following the MCAO/R or sham-operation, three different motor function tests were conducted (neurological deficit scoring, grip strength test, and inverted screen test; n=10 per each group) and mice were immediately sacrificed for further experimentation. DHE, dihydroethidium; MCAO/R, middle cerebral artery occlusion and reperfusion; PSL, leaf extract of *Platycarya strobilacea*; PSL-H, pretreated with high doses of PSL; PSL-L, pretreated with low doses of PSL; ROS, reactive oxygen species; TUNEL, terminal deoxynucleotidyl transferase dUTP nick end labeling; VEH, pretreated with distilled water and subjected to MCAO/R.

MCAO/R

Mice were anesthetized with an intraperitoneal injection of 30 mg/kg ketamine and 20 mg/kg xylazine cocktail. Following a midline neck incision, the left common carotid artery (CCA) and the external carotid artery were ligated. A clip was placed on the internal carotid artery (ICA) to prevent bleeding. After creating a small hole in the CCA, 7-0 nylon monofilament with a round silicon-coated tip (0.2 mm in diameter) was inserted into the hole. Following removal of the clip at the ICA, the silicon-coated filament was further inserted into the ICA to occlude the middle cerebral artery (MCA) until the cerebral blood flow (CBF) was abruptly dropped. When CBF dropped below 20% of the baseline, insertion of the filament was stopped and 60 minutes of occlusion began. After 60 minutes, the filaments were withdrawn and reperfusion began. During the operation, CBF and rectal temperature (37°C±0.5°C) were carefully monitored using a Doppler flowmeter (Periflux 5000, Perimed AB, Stockholm, Sweden) and heating pad, respectively. Sham-operated mice underwent the same surgical procedure, except that the filament was not advanced far enough to occlude the MCA.

In vivo ROS detection assay

To detect brain cellular ROS accumulation we used dihydroethidium (DHE), which is a fluorescent ROS probe. For this procedure, 10 mg/kg of DHE (Invitrogen, Carlsbad, CA, USA) was diluted in 50 μL of normal saline and injected into the mice (n=2 per each group) via a jugular vein just before

MCAO/R. At 2 hours after MCAO/R, the brain hemisphere ipsilateral to fCI lesion was removed, immersed in 30% sucrose solution for cryopreservation, embedded in an OCT compound, and frozen in dry ice. Using a cryostat microtome (HM430, Leica, Walldorf, Germany) set at –21°C, a total of 10 coronal sections (50 μm in thickness, between –0.1 and +0.4 mm from bregma) were obtained from each mouse. Four randomly selected sections from each mouse were counterstained with Hoechst 33258 (Santa Cruz Biotechnology, Dallas, TX, USA) for 5 minutes at 24°C and a coverslip was placed on each slide. The resulting DHE fluorescence was photographed under a laser scanning confocal microscope (LSM700, Zeiss, Munchen, Germany) at 400× and the fluorescence intensity in the high-power field (HPF) was determined using Image analyzer (ImageJ 1.37v, National Institutes of Health, Bethesda, MD, USA). The mean fluorescence intensity was averaged per group.

Neurological deficit scoring

As the first tool for assessing the motor deficits, the neurological deficit scoring (NDS) was employed in accordance with a previous study [26]. In brief, 24-hour post-MCAO/R, motor functions in the mice (n=10 per group) were tested using a scoring scale consisting of 4 points: 0, no neurologic deficit; 1, failure to spread out affected forepaw; 2, unidirectional circling; 3, falling to one side; and 4, no voluntary movement. The NDS was performed by two investigators blinded to the study and the scores were averaged per group.

Grip strength test

The second tool for assessing the motor deficits, the grip strength test, was employed in accordance with a previous study [27]. In brief, after completing the NDS, mice (n=10 per group) were placed on a wire grid attached to custom-made grip test box and allowed to grab the grid with both forepaws before being gently pulled until they released their grip. The maximum force generated was recorded in grams. All tests were conducted in triplicates and the values recorded were averaged per group.

Inverted screen test

The third tool for assessing motor deficits, the inverted screen test, was employed in accordance with a previous study [28]. In brief, after completing the grip strength test, each mouse (n=10 per group) was placed on a custom-made metal grid screen. After placement, the mice were allowed to grip the grid and the screen was inverted to 180° over a cage containing bedding. Latency to fall was recorded up to 180 seconds, and the trials were conducted in triplicates. The values were averaged per group.

Infarct volume measurement

After finishing all the motor function tests, a whole brain of each mouse (n=4 per group) was obtained and cut into eight coronal slices with 1 mm thickness using a brain matrix (Zivic Instruments, Pittsburgh, PA, USA). The sections were stained with 2% of 2,3,5-triphenyltetrazolium chloride (TTC; Sigma, St. Louis, MO, USA) diluted in phosphate-buffered saline (PBS) for 17 minutes at 37°C. The TTC-stained tissues were photographed and ischemic sided brain cortices were immediately isolated and stored at –80°C until further use in western blotting. The ipsilateral infarct volume was analyzed by an observer blinded to the study with the aid of Image J. To correct the effects of brain edema, the ipsilateral infarcted area in each section was normalized to the contralateral side and expressed as percentage of the contralateral hemisphere. The infarcted areas in each section were summed and averaged per group.

Histologic preparation

After finishing all the motor function tests, the mice (n=6 per group) were anesthetized with an intraperitoneal injection of chloral hydrate (30 mg/kg) and transcardially perfused with 4% paraformaldehyde. Post fixation, each coronal section between –1 and +1 mm from the bregma were trimmed out with the aid of a brain matrix and dehydrated by placing the tissues in an alcohol series. The tissues were then cleared with xylene and embedded in paraffin following which, 5-μm-thick sections were made by a tissue microtome (RM2255, Leica) and mounted on microscope slides. The resulting "sets" for each mouse that contained at least 50 slides, were stored at 24°C until further use in different experiments, such as, the terminal deoxynucleotidyl transferase dUTP nick end labeling (TUNEL) assay or immunohistochemistry (IHC).

TUNEL assay

The TUNEL assay was conducted by using a commercial kit (DeadEnd, Promega, Madison, WI, USA). According to the manufacturer' protocol, two slides randomly selected from an individual set were assayed and the TUNEL-positive cells of ischemic lesions in at least three randomly chosen HPF were counted under the light microscope (DM4, Leica) at ×400. The counts were averaged per group.

Immunohistochemistry

Each of the two slides randomly selected from an individual set were subjected to an antigen retrieval and endogenous peroxidase quenching step in accordance with a previous study [29]. Next, the slides were incubated overnight with rabbit antibodies against 4-hydroxynonenal (4-HNE), 8-hydroxyl-2'-deoxyguanosine (8-OHdG), and cleaved caspase-3 diluted in PBS at a ratio of 1:200 at 4°C. The slides were then incubated with anti-rabbit IgG diluted in PBS at a ratio of 1:200 for 2 hours at 24°C. All antibodies were purchased from Abcam (Cambridge, UK). Next, the sections were incubated with avidin-biotin complex (Vector, Burlingame, CA, USA) for 1 hour at 24°C. The resulting immunoreactivities were detected using a chromogen, 3,3'-diaminobenzidine tetrahydrochloride (Sigma-Aldrich). After mounting with coverslips, the immunopositive cells in at least three randomly chosen HPF were counted under the light microscope at ×400. The counts were averaged per group.

Western blot

To quantify the level of different antioxidative enzymes, western blot was employed. The lesion-bearing cortices (n=4 per group) that had been stored at –80°C previously, were homogenized and centrifuged at 120 ×g at 4°C for 10 minutes. Using a commercially available kit (BCA protein assay kit, Pierce, Rockford, IL, USA), the total protein concentrations were measured in accordance with the manufacturer's
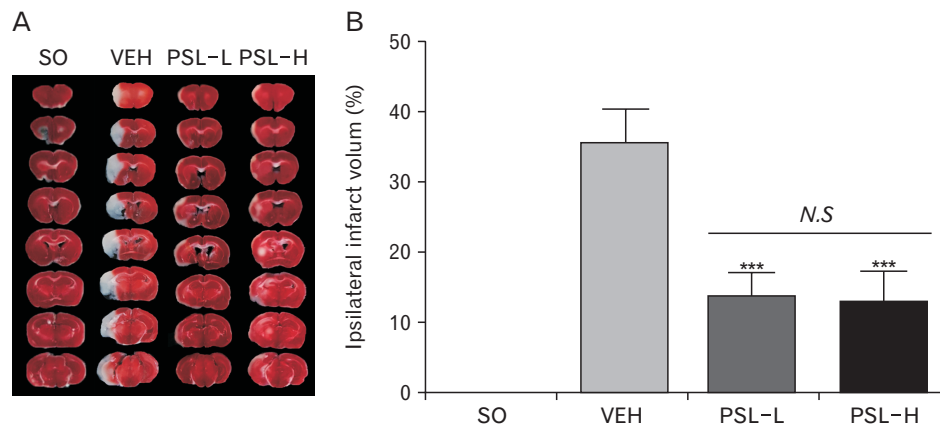
Fig. 2. Effects of PSL on infarct volume in a mouse model of focal cerebral ischemia. (A) Representative photographs showing the TTC-stained brain serial sections of the different groups. Upon the TTC staining, infarcted areas appear generally white in color. (B) Quantitation graphs showing the % area of infarction (n=4 per group, ***$P<0.001$ vs. VEH). Data were represented as mean±SEM. N.S, statistically not significant between indicated groups. PSL, leaf extract of *Platycarya strobilacea*; TTC, 2,3,5-triphenyltetrazolium chloride; PSL-H, pretreated with high doses of PSL; PSL-L, pretreated with low doses of PSL; SO, a group subjected to a sham-operation; VEH, pretreated with distilled water and subjected to middle cerebral artery occlusion and reperfusion.

protocol. Thereafter, the protein samples were separated by 10% sodium dodecyl sulfate gel and transferred onto a polyvinylidene difluoride membrane (Bio-Rad, Hercules, CA, USA), which was blocked with 5% skim milk diluted in Tris-buffered saline with 0.1% Tween 20 (TBS-T) for 40 minutes at 24°C. The membranes were incubated with rabbit antibodies against superoxide dismutase (SOD), glutathione peroxidase (GPX), heme oxygenase-1 (HO-1), and β-actin diluted in TBS-T at a ratio of 1:1,000 at 4°C overnight. After washing, the membranes were incubated with anti-rabbit IgG diluted in TBS-T at a ratio of 1:1,000 for 2 hours at 4°C. All antibodies were purchased from Abcam (Abcam). The resulting immunoreactivities were visualized using a chemiluminescence detection system (Immobilon Western, Millipore, Burlington, MA, USA) and photographed using an imaging device (Chemi-doc, Davinch-K, Seoul, Korea). The band intensities were quantified by ImageJ and the results were normalized using β-actin as a house-keeping control. The values were averaged per group.

Statistical analysis

All data were presented as mean±standard error of the mean. Comparisons of the data from the different groups were performed with one-way analysis of variance (ANOVA, PASW Statistics version 18, SPSS Inc., Chicago, IL, USA). Differences with P-values of <0.05 were considered statistically significant. Each "n" value refers to the number of animals.

Results

PSL diminishes fCI-induced infarct volume and behavioral deficits

As shown in TTC-stained tissues (Fig. 2A), there were no visible areas of infarction in the SO group as expected. However, at 24 hours after MCAO/R, the VEH group exhibited marked areas of infarction. The ipsilateral infarct volumes in both the PSL-L and the PSL-H groups were approximately 1/3 of that of the VEH group (13.3±3.6 and 12.9±4.5 vs. 35.5±4.8%, respectively; $P<0.001$) (Fig. 2B) and the extent of their reduction was not statistically different between these groups. Three different behavioral tests were conducted to assess the role of PSL on fCI-associated motor deficits. First, NDS demonstrated that the motor deficits of the VEH group were prominent (Fig. 3A). However, both the PSL-L and PSL-H groups exhibited significantly improved motor function compared with the VEH group (1.9±0.7 and 1.9±0.7 vs. 2.7±0.9; $P<0.01$). Second, the grip strength test revealed that grip strength of the VEH group was significantly weakened ($P<0.001$ vs. SO) (Fig. 3B). Inversely, both the PSL-L and PSL-H groups exhibited significantly higher values in terms of grip strength compared with the VEH group (108.1±18.6 and 139.8±19.6 vs. 76.7±14.6, respectively; $P<0.001$), and the increase was dose-dependent ($P<0.01$). Third, the inverted screen test showed that the latencies to fall were significantly reduced in the VEH group compared with the SO group (19.0±14.1 vs. 167.9±15.0; $P<0.001$) (Fig. 3C). However, the groups treated with PSL remained on
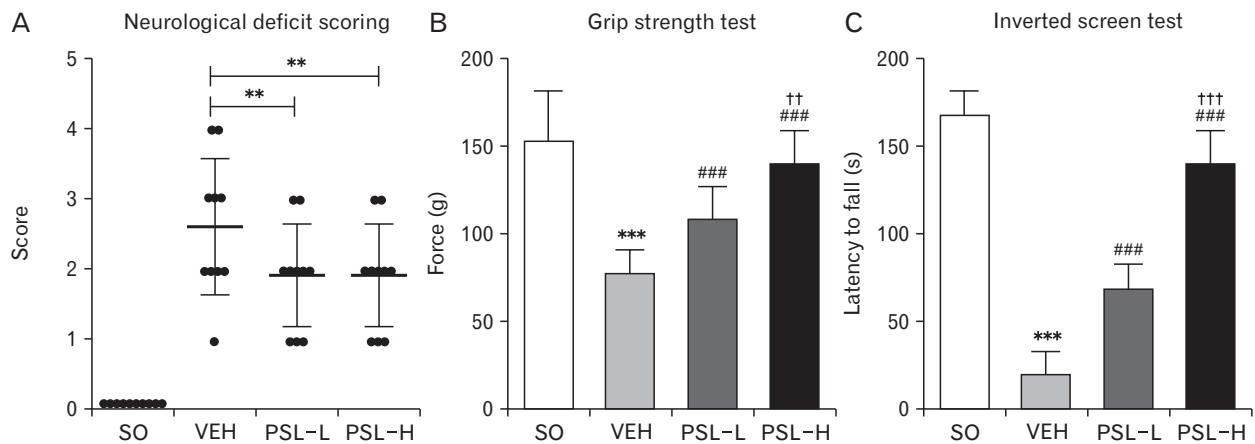
Fig. 3. Effects of PSL on motor deficits in a mouse model of focal cerebral ischemia. (A) Graph showing the neurological deficit scores of the different groups performed 24 hours after the operation. Dots indicate individual scores. (B) Quantitative graphs showing the results of the grip strength test and (C) the inverted screen test. Data are represented as mean±SEM (n=10 per each group; ***$P<0.001$ vs. SO; ###$P<0.001$ vs. VEH; ††$P<0.01$ and †††$P<0.001$ vs. PSL-L). PSL, leaf extract of *Platycarya strobilacea*; PSL-H, pretreated with high doses of PSL; PSL-L, pretreated with low doses of PSL; SO, a group subjected to a sham-operation; VEH, pretreated with distilled water and subjected to middle cerebral artery occlusion and reperfusion.
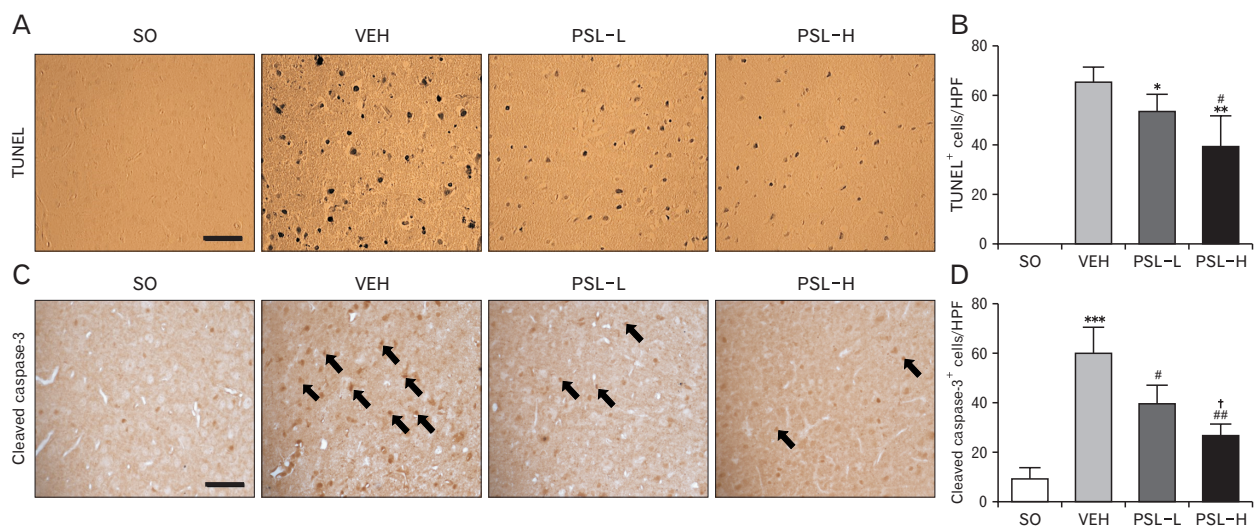

Fig. 4. Effects of PSL on cellular apoptosis in the ischemic cortex of a mouse model of focal cerebral ischemia. Representative images of TUNEL stained ischemic cortices (A) and quantitative graph showing the number of TUNEL-positive (TUNEL+) cells in the cortical lesions of mice of different groups (n=6 per each group; *$P<0.05$ and **$P<0.01$ vs. VEH; #$P<0.05$ vs. PSL-L) (B). Representative images of immunohistochemistry using the cleaved caspase-3 antibody (arrows indicates cleaved caspase-3+ cells) (C) and the quantitative graph showing the number of cleaved caspase-3+ cells in cortical lesions of mice in the different groups (n=6 per each group; ***$P<0.001$ vs. SO; #$P<0.05$ and ##$P<0.01$ vs. VEH; †$P<0.05$ vs. PSL-L) (D). Scale bar=50 μm. All data are represented as mean±SEM in a randomly chosen HPF. HPF, high-power field; PSL, leaf extract of *Platycarya strobilacea*; PSL-H, pretreated with high doses of PSL; PSL-L, pretreated with low doses of PSL; SO, a group subjected to a sham-operation; TUNEL, terminal deoxynucleotidyl transferase dUTP nick end labeling; VEH, pretreated with distilled water and subjected to middle cerebral artery occlusion and reperfusion.

the inverted screen longer than VEH group (68.0±14.5 and 140.2±17.4 in PSL-L and -H group, respectively; $P<0.001$) and this response was dose-dependent ($P<0.001$). These findings demonstrated that PSL could reduce the infarct volume and improve the motor deficits seen in fCI mice.

PSL attenuates fCI-induced brain cortical apoptosis

TUNEL staining and IHC detection of cleaved caspase-3, a protein involved in the execution of cellular apoptosis, was employed to assess the extent of cellular apoptosis in brain cortex at 24-hour post-MCAO/R. As shown in Fig. 4A and

B, no TUNEL-positive apoptotic cells were detected in brain cortical parenchyma of the SO group as expected. However, presence of TUNEL-positive cells was prominent in the VEH group. In contrast, the number of TUNEL-positive cells was significantly reduced in the groups supplemented with PSL compared with the VEH group (53.5 ± 7.0 and 38.5 ± 13.2 in PSL-L and -H group, respectively, vs. 65.1 ± 6.3; $P<0.05$ and $P<0.01$) and this decrease was dose-dependent ($P<0.05$). Additionally, as shown in Fig. 4C and D, the number of the cleaved caspase-3-immunoreactive cells (indicated by arrows in Fig. 4C) in the ischemic cortex was significantly increased in the VEH group by approximately 6-fold compared with the SO group (59.8 ± 10.6 vs. 9 ± 4.4; $P<0.001$). However, when compared with the VEH group, the numbers of cleaved caspase-3-immunoreactive cells in the ischemic cortex were markedly decreased in PSL-supplemented groups (39.2 ± 7.8 and 26.4 ± 4.8 in PSL-L and -H group, respectively; $P<0.05$ and $P<0.01$) and the inter-group difference was significant
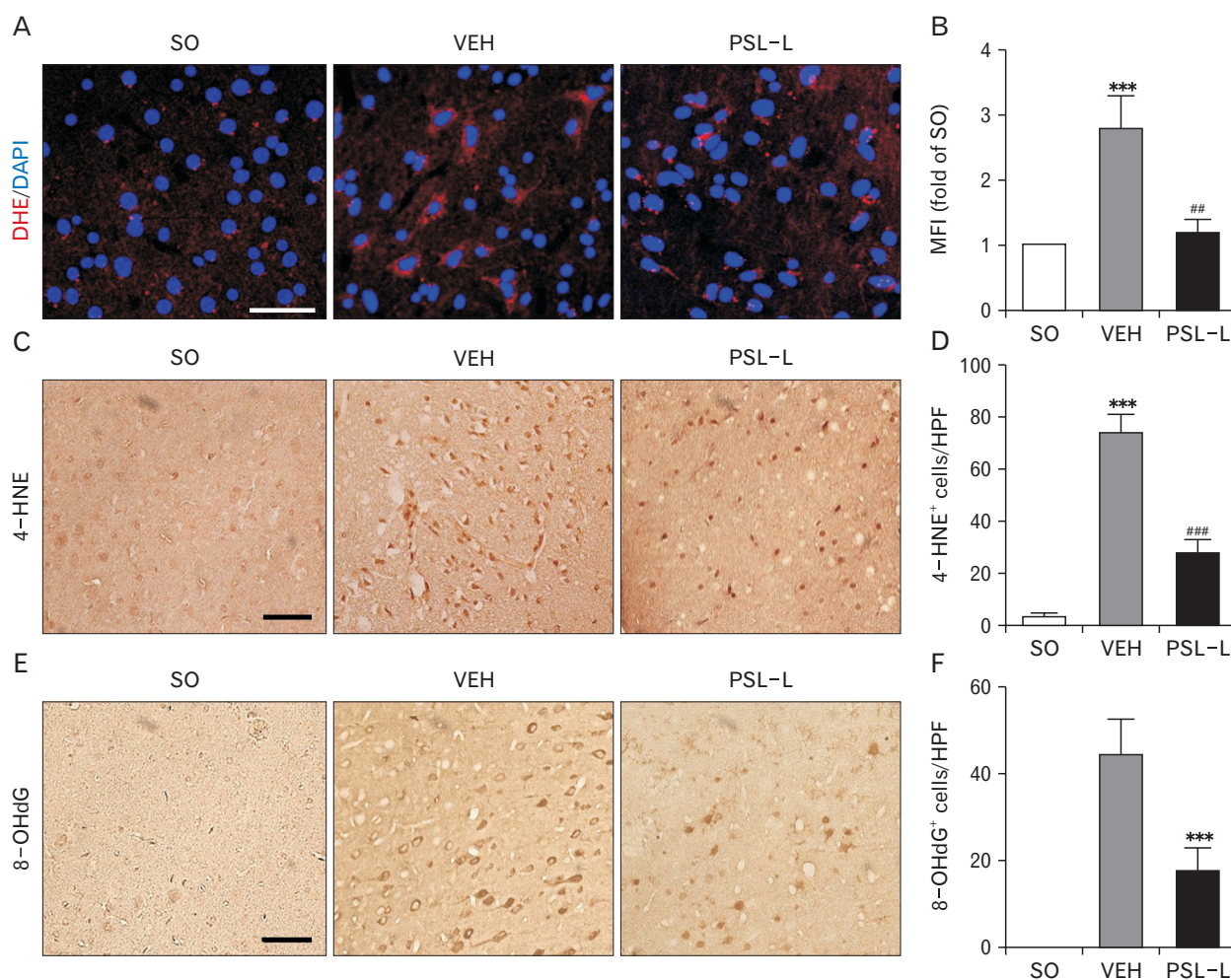
Fig. 5. Effects of 20 mg/kg PSL on intracellular ROS accumulation in the ischemic cortex of a mouse model of focal cerebral ischemia. For this experiment, 10 mg/kg of DHE was injected into the mice via a jugular vein just before the operation. Representative images showing the cortical DHE fluorescence (red) acquired at 2 hours after the operation (scale bar=100 μm) (A) and the quantitative graphs (n=2 per each group; ***$P<0.001$ vs. SO; ##$P<0.01$ vs. VEH) (B). Data were represented as MFI±SEMs. Representative images of 4-HNE–immunostained ischemic cortices (scale bar=50 μm) (C) and the quantitative graph showing the numbers of 4-HNE–immunopositive (4-HNE+) cells (n=6 per each group; ***$P<0.001$ vs. SO; ###$P<0.001$ vs. VEH) (D). Representative images of 8-OHdG-immunostained ischemic cortices (scale bar=50 μm) (E) and the quantitative graph showing the numbers of 8-OHdG-immunopositive (8-OHdG+) cells (n=6 per each group; ***$P<0.001$ vs. VEH) (F). All data in (D) and (F) are represented as mean±SEM in a randomly chosen HPF. DHE, dihydroethidium; HPF, high-power field; MFI, mean fluorescence intensity; PSL, leaf extract of *Platycarya strobilacea*; HPF, high-power field; PSL-L, pretreated with low doses of PSL; ROS, reactive oxygen species; SO, a group subjected to a sham-operation; VEH, pretreated with distilled water and subjected to middle cerebral artery occlusion and reperfusion; 4-HNE, 4-Hydroxynonenal; 8-OHdG, 8-Hydroxyl-2'-deoxyguanosine.

(P<0.05). These data suggest that the PSL-induced protection against fCI involves an attenuation of cellular apoptosis.

PSL attenuates fCI-associated oxidative damages

Having established that PSL, even at a low level (20 mg/kg), can reduce the fCI-associated phenotypes, we performed further studies to reveal the underlying mechanism using only the PSL-L group as the treatment group. Given that, a vast majority of phytochemicals are known to exert their beneficial roles on the cellular level via an antioxidant mechanism, we employed *in vivo* staining with DHE. DHE is a well-known superoxide marker used to identify whether the antioxidant activity is the underlying mechanism of PSL-induced neuroprotection. As shown in Fig. 5A and B, brain ROS accumulation (red fluorescence) was abruptly increased by 2-hour post-fCI insult in the VEH group (2.8±0.5, P<0.001). Conversely, the PSL-L group exhibited a marked reduction of DHE-fluorescence when compared with the VEH group (1.2±0.2, P<0.01). Given that lipid peroxidation and DNA damage are commonly associated with ROS accumulation, we next quantified these mechanisms of damage by employing immunohistochemical detection of 4-HNE and 8-OHdG, which are markers of lipid peroxidation and DNA damage, respectively. As shown in Fig. 5C–F, the results revealed that both 4-HNE– and 8-OHdG–immunopositive stained cells were significantly increased in the brain cortices of the VEH group compared with the SO group (74.0±7.2 for 4-HNE, P<0.001; 44.0±8.5 for 8-OHdG). However, the PSL-L group exhibited a marked reduction in these values when compared with the VEH group (27.8±5.2 for 4-HNE, P<0.001; 17.6%±5.4% for 8-OHdG, P<0.001). Together, these results suggest that PSL can attenuate the fCI-induced ROS accumulation and the subsequent oxidative damage, such as, lipid peroxidation and DNA damage, in brain cells.

PSL supplement can augment the expression level of an antioxidative enzyme, HO-1

To identify the possible modulation of PSL on brain cellular antioxidative enzyme levels in fCI mice, the protein levels of three enzymes, SOD, GPX, and HO-1, were quantified by western blot technique. As illustrated by the representative band images (Fig. 6A) and the quantification graphs (Fig. 6B–
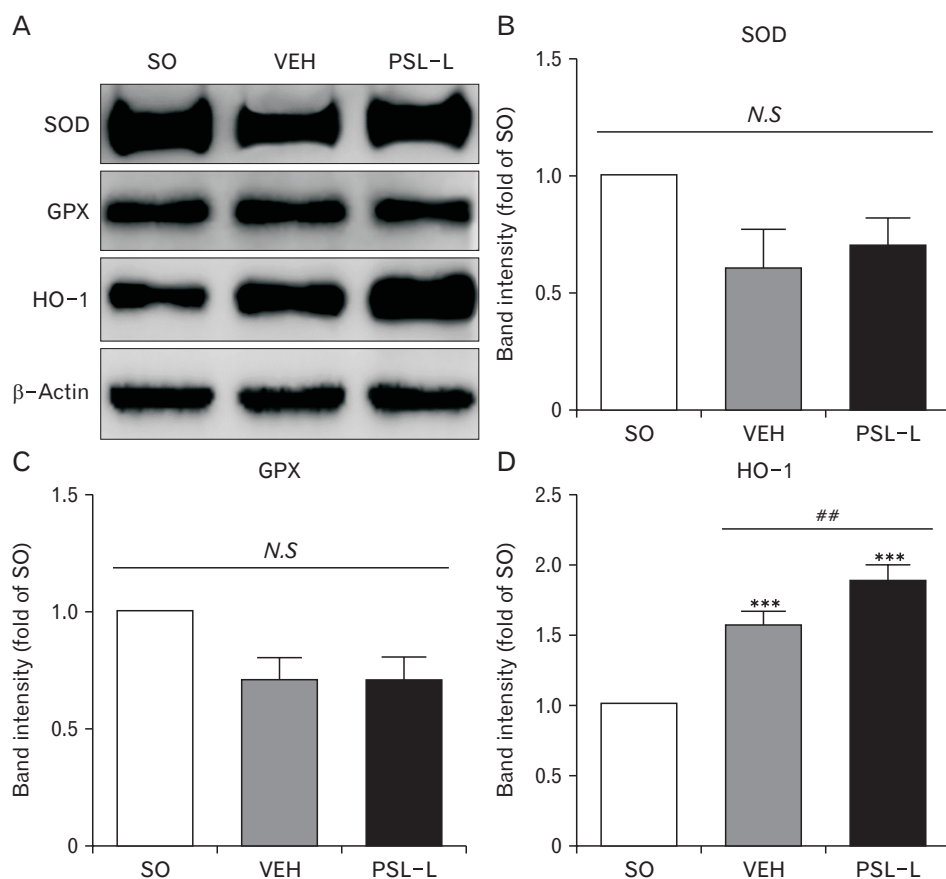

Fig. 6. Effects of 20 mg/kg PSL on changes in the ischemic cortical expression of antioxidant enzymes in a mouse model of focal cerebral ischemia. (A) Representative western blot bands for assessing the amount of SOD, GPX, and HO-1 in the ischemic cortical homogenates of the indicated groups and (D) the quantitative graphs showing the band intensities of SOD (B), GPX (C), and HO-1 (D). β-actin was used as a loading control. All data are represented as mean±SEM (n=4 per each group; ***P<0.001 vs. SO; ##P<0.01 vs. VEH). GPX, glutathione peroxidase; HO-1, heme oxygenase-1; *N.S*, statistically not significant between indicated groups; PSL, leaf extract of *Platycarya strobilacea*; PSL-L, pretreated with low doses of PSL; SO, a group subjected to a sham-operation; SOD, superoxide dismutase; VEH, pretreated with distilled water and subjected to middle cerebral artery occlusion and reperfusion.

D), the expression levels of SOD and GPX in the ischemic lesion remained unchanged in all the groups. Notably, the levels of HO-1 were significantly increased in the VEH and PSL-L groups compared with the SO group (1.5±0.1 and 1.9±0.1; $P<0.001$) and the increment was significantly exaggerated in that of PSL-L group ($P<0.01$). This result suggests that HO-1 can be upregulated by the compensatory response in fCI brain tissue and PSL may further reinforce the upregulation. This finding suggests that upregulation of HO-1, at least in part, may contribute to the neuroprotection of PSL against fCI by reducing oxidative damage.

Discussion

The fCI begins with a permanent or transient insufficiency of cerebral blood flow in the focal brain region. This induces deprivation of oxygen and nutrient supply to brain tissues, leading to an energy failure combined with accumulation of toxic substances [30]. Among these, ROS such as superoxide radicals are known as key molecules that could eventually result in neuronal death [31]. In healthy people, a balance is maintained between ROS production and elimination, which is mediated by the antioxidant enzyme system that is primarily composed of SOD, GPX, and HO-1 [32]. However, the fCI, once initiated, triggers the overproduction of ROS by multiple pathological cascades. The resulting ROS overload in turn threatens neuronal survival owing to their ability to propagate the initial attack on lipid-rich neuronal membranes, causing lipid peroxidation that subsequently results in DNA damage [33]. Accordingly, upregulation of intrinsic neuronal antioxidant enzymes may be an important target for developing fCI therapeutics.

It is well-known that polyphenol compounds, that naturally-occurring plants are enriched with, can combat oxidative stress by upregulation of various endogenous antioxidant enzymes and thus may protect humans against oxidative stress-related pathologies including hypoxia- and inflammation-related diseases [34]. Among the natural plants that are known to trigger this upregulation, PS leaf extract is known to contain several polyphenolic compounds e.g., ellagic acid, gallic acid, and juglone [35-37]. As such, it has attracted significant scientific attention [38]. In spite of accumulating evidence that suggest the role of individual compounds of PSL on the activation of antioxidant enzyme-mediated defense system, only limited information is available on the role of PSL itself.

To the best of our knowledge, this study is the first to demonstrate that a PSL supplement can attenuate fCI-induced brain cellular injury via an upregulation of HO-1. This suggests a possible therapeutic mechanism. These findings are consistent with previous studies [39, 40]. For example, it has been previously reported that neuronal expression of HO-1 is usually detected in rodent brains challenged with anoxic stimuli, including hypoxia or oxidative stress [41]. Furthermore, genetically engineered HO-1–deficient mice exhibit exaggeration in ischemic damage when compared to wild type controls [42, 43]. Together with the results of this study, these findings suggest that PSL possesses a powerful neuroprotective effect, which may be effective against cerebral ischemia via upregulation of HO-1.

To date, our studies have only focused on identifying the roles of the PSL therapeutic effect against fCI injury *in vivo*. As such, we have not yet addressed the upstream signal pathway of HO-1 activation that is involved in PSL-mediated neuroprotection. The nuclear factor erythroid-derived 2-related factor 2 (Nrf2) is the master regulator of antioxidative enzymes including HO-1, and Nrf2 is strongly suspected to be one of the most powerful candidates for upstream targeting [44]. Under healthy conditions, a cytosolic Nrf2 is sequestered by binding to Kelch-like ECH-associated protein 1 (Keapl), which inhibits translocation into the nucleus [45]. Several forms of stimuli trigger the conformational change of Keapl that enables the Nrf2/Keap1 complex to release Nrf2, which then translocates to the nucleus and binds to antioxidant-related elements in the promoter regions of antioxidant genes [46]. Additionally, several signaling cascades such as mitogen-activated protein kinase, protein kinase C, and phosphatidylinositol 3-kinase (PI3K/Akt) are involved in the phosphorylation of Nrf2 as well as its nuclear translocation [47]. Hundreds of reports provide evidence for the role of various polyphenols on the activation of Nrf2 [48-50]. It is noteworthy that that ellagic acid [51], gallic acid [52], and juglone [53] have been demonstrated to activate the Nrf2/ARE/HO-1 cascade. These reports lead us to assume that the activation of the Nrf2/ARE/HO-1 cascade is mediated by the major components of PSL as described above, that induces a neuroprotective effect during and after fCI. More detailed analysis of the signaling pathways underlying the neuroprotective action of PSL, e.g., the Nrf2/ARE/HO-1 cascade, is important during further investigations.

In conclusion, we revealed that PSL pretreatment can attenuate the infarct volume and improve sensorimotor deficit followed by fCI by exerting antioxidative efficacy. In this re-

gard, we strongly suggest that PSL supplement can be a useful preventive strategy against ischemic stroke.

ORCID

Ji Hye Lee: http://orcid.org/0000-0002-1570-3425

Ji Heun Jeong: http://orcid.org/0000-0002-3439-8825

Young-Gil Jeong: http://orcid.org/0000-0001-8696-107X

Do-Kyung Kim: http://orcid.org/0000-0001-6655-7061

Nam-Seob Lee: http://orcid.org/0000-0001-6817-5403

Chun Soo Na: http://orcid.org/0000-0003-0166-8574

Eun Soo Doh: http://orcid.org/0000-0002-4556-5377

Seung Yun Han: http://orcid.org/0000-0002-7055-6341

Author Contributions

Conceptualization: JHL, SYH, YGJ, NSL, ESD. Data acquisition: JHL, CSN. Data analysis or interpretation: JHL, JHJ, DKK. Drafting of the manuscript: JHL, SYH. Critical revision of the manuscript: SYH, JHJ. Approval of the final version of the manuscript: all authors.

Conflicts of Interest

No potential conflict of interest relevant to this article was reported.

Acknowledgements

References

1. Bonita R, Beaglehole R, Asplund K. The worldwide problem of stroke. Curr Opin Neurol 1994;7:5-10.
2. Lee RH, Lee MH, Wu CY, Couto E Silva A, Possoit HE, Hsieh TH, Minagar A, Lin HW. Cerebral ischemia and neuroregeneration. Neural Regen Res 2018;13:373-85.
3. Lawson TR, Brown IE, Westerkam DL, Blackhurst DW, Sternberg S, Leacock R, Nathaniel TI. Tissue plasminogen activator (rt-PA) in acute ischemic stroke: outcomes associated with ambulation. Restor Neurol Neurosci 2015;33:301-8.
4. Tekle WG, Chaudhry SA, Hassan AE, Peacock JM, Lakshminarayan K, Tsai A, Luepker R, Anderson DC, Qureshi AI. Utilization of intravenous thrombolysis in 3-4.5 hours: analysis of the Minnesota stroke registry. Cerebrovasc Dis 2012;34:400-5.
5. Li W, Suwanwela NC, Patumraj S. Curcumin prevents reperfu-

sion injury following ischemic stroke in rats via inhibition of NF κB, ICAM-1, MMP-9 and caspase-3 expression. Mol Med Rep 2017;16:4710-20.
6. He X, Deng FJ, Ge JW, Yan XX, Pan AH, Li ZY. Effects of total saponins of Panax notoginseng on immature neuroblasts in the adult olfactory bulb following global cerebral ischemia/reperfusion. Neural Regen Res 2015;10:1450-6.
7. Sunwoo YY, Park SI, Chung YA, Lee J, Park MS, Jang KS, Maeng LS, Jang DK, Im R, Jung YJ, Park SA, Kang ES, Kim MW, Han YM. A pilot study for the neuroprotective effect of Gongjin-dan on transient middle cerebral artery occlusion-induced ischemic rat brain. Evid Based Complement Alternat Med 2012;2012: 682720.
8. Lu W, Xv L, Wen J. Protective effect of extract of the Camellia japonica L. on cerebral ischemia-reperfusion injury in rats. Arq Neuropsiquiatr 2019;77:39-46.
9. Yang H, Zhang A, Zhang Y, Ma S, Wang C. Resveratrol pretreatment protected against cerebral ischemia/reperfusion injury in rats via expansion of t regulatory cells. J Stroke Cerebrovasc Dis 2016;25:1914-21.
10. Yan RY, Wang SJ, Yao GT, Liu ZG, Xiao N. The protective effect and its mechanism of 3-n-butylphthalide pretreatment on cerebral ischemia reperfusion injury in rats. Eur Rev Med Pharmacol Sci 2017;21:5275-82.
11. Landete JM. Ellagitannins, ellagic acid and their derived metabolites: a review about source, metabolism, functions and health. Food Res Int 2011;44:1150-60.
12. Fang F, Qin Y, Qi L, Fang Q, Zhao L, Chen S, Li Q, Zhang D, Wang L. Juglone exerts antitumor effect in ovarian cancer cells. Iran J Basic Med Sci 2015;18:544-8.
13. Ahmad T, Suzuki YJ. Juglone in oxidative stress and cell signaling. Antioxidants (Basel) 2019;8:E91.
14. Rozentsvit A, Vinokur K, Samuel S, Li Y, Gerdes AM, Carrillo-Sepulveda MA. Ellagic acid reduces high glucose-induced vascular oxidative stress through ERK1/2/NOX4 signaling pathway. Cell Physiol Biochem 2017;44:1174-87.
15. Chen P, Chen F, Zhou B. Antioxidative, anti-inflammatory and anti-apoptotic effects of ellagic acid in liver and brain of rats treated by D-galactose. Sci Rep 2018;8:1465.
16. Ji Y, Qu Z, Zou X, Ji C. Effects of juglone on ROS production and mitochondrial transmembrane potential in SGC-7901 cells. In: 2010 4th International Conference on Bioinformatics and Biomedical Engineering; 2010 Jun 18-20; Chengdu, China. Piscataway, NJ: Institute of Electrical and Electronics Engineers; 2010.
17. Costantino S, Paneni F, Lüscher TF, Cosentino F. Pin1 inhibitor Juglone prevents diabetic vascular dysfunction. Int J Cardiol 2016;203:702-7.
18. Rodrigo R, Fernández-Gajardo R, Gutiérrez R, Matamala JM, Carrasco R, Miranda-Merchak A, Feuerhake W. Oxidative stress and pathophysiology of ischemic stroke: novel therapeutic opportunities. CNS Neurol Disord Drug Targets 2013;12:698-714.
19. Lee JH, Kim H, Shim JH, Park J, Lee SK, Park KK, Chung WY. *Platycarya strobilacea* leaf extract inhibits tumor necrosis factor-

αproduction and bone loss induced by *Porphyromonas gingivalis*-derived lipopolysaccharide. Arch Oral Biol 2018;96:46-51.

20. Kim EJ, Choi JY, Park BC, Lee BH. Platycarya strobilacea S. et Z. Extract has a high antioxidant capacity and exhibits hair growth-promoting effects in male C57BL/6 mice. Prev Nutr Food Sci 2014;19:136-44.

21. Zhang L, Wang Y, Xu M. *In vitro* antitumor activities of *Platycarya strobilacea* Sieb et Zucc infructescence extracts. Trop J Pharm Res 2014;13:849-54.

22. Zhang LL, Wang YM, Xu M. Preparation and antimicrobial activity of tannin polymers from *Platycarya strobilacea* infructescence. Mater Res Innov 2014;18:S2-1046-S2-1049.

23. El Hadrami A, Kone D, Lepoivre P. Effect of juglone on active oxygen species and antioxidant enzymes in susceptible and partially resistant banana cultivars to black leaf streak disease. Eur J Plant Pathol 2005;113:241-54.

24. Han DH, Lee MJ, Kim JH. Antioxidant and apoptosis-inducing activities of ellagic acid. Anticancer Res 2006;26:3601-6.

25. National Research Council of the National Academies. Guide for the care and use of laboratory animals. 8th ed. Washington, DC: The National Academies Press; 2011.

26. Longa EZ, Weinstein PR, Carlson S, Cummins R. Reversible middle cerebral artery occlusion without craniectomy in rats. Stroke 1989;20:84-91.

27. Takeshita H, Yamamoto K, Nozato S, Inagaki T, Tsuchimochi H, Shirai M, Yamamoto R, Imaizumi Y, Hongyo K, Yokoyama S, Takeda M, Oguro R, Takami Y, Itoh N, Takeya Y, Sugimoto K, Fukada SI, Rakugi H. Modified forelimb grip strength test detects aging-associated physiological decline in skeletal muscle function in male mice. Sci Rep 2017;7:42323.

28. Drapeau E, Riad M, Kajiwara Y, Buxbaum JD. Behavioral phenotyping of an improved mouse model of Phelan-McDermid syndrome with a complete deletion of the shank3 gene. eNeuro 2018;5:ENEURO.0046-18.2018.

29. Jeong JH, An JH, Yang H, Kim DK, Lee NS, Jeong YG, Na CS, Na DS, Dong MS, Han SY. Protective effect of Rhus verniciflua Stokes extract in an experimental model of post-menopausal osteoporosis. Anat Cell Biol 2017;50:219-29.

30. Mir MA, Al-Baradie RS, Alhassainawi MD. Recent advances in stroke therapeutics. Hauppauge, NY: Nova Science Publishers; 2014. p.25-80.

31. Duris K, Rolland WB, Zhang JH. Stroke pathophysiology and reactive oxygen species. In: Laher I, editor. Systems Biology of Free Radicals and Antioxidants. Berlin: Springer; 2014. p.1979-97.

32. Olmez I, Ozyurt H. Reactive oxygen species and ischemic cerebrovascular disease. Neurochem Int 2012;60:208-12.

33. Tsai CC, Wu SB, Cheng CY, Kao SC, Kau HC, Chiou SH, Hsu WM, Wei YH. Increased oxidative DNA damage, lipid peroxidation, and reactive oxygen species in cultured orbital fibroblasts from patients with Graves' ophthalmopathy: evidence that oxidative stress has a role in this disorder. Eye (Lond) 2010;24:1520-5.

34. Zhang H, Tsao R. Dietary polyphenols, oxidative stress and antioxidant and anti-inflammatory effects. Curr Opin Food Sci 2016;8:33-42.

35. Zhang LL, Xu M, Wang YM, Wu DM, Chen JH. Optimizing ultrasonic ellagic acid extraction conditions from infructescence of *Platycarya strobilacea* using response surface methodology. Molecules 2010;15:7923-32.

36. Maoyi W, Jungtian L, Ning H. Determination of gallic acid in *Platycarya strobilacea* Sieb. et Zucc by RP-HPLC. China Pharm 2010;3:378-9.

37. Nour V, Trandafir I, Cosmulescu S. HPLC determination of phenolic acids, flavonoids and juglone in walnut leaves. J Chromatogr Sci 2013;51:883-90.

38. Altemimi A, Watson DG, Kinsel M, Lightfoot DA. Simultaneous extraction, optimization, and analysis of flavonoids and polyphenols from peach and pumpkin extracts using a TLC-densitometric method. Chem Cent J 2015;9:39.

39. Bajpai VK, Alam MB, Quan KT, Kwon KR, Ju MK, Choi HJ, Lee JS, Yoon JI, Majumder R, Rather IA, Kim K, Lee SH, Na M. Antioxidant efficacy and the upregulation of Nrf2-mediated HO-1 expression by (+)-lariciresinol, a lignan isolated from Rubia philippinensis, through the activation of p38. Sci Rep 2017;7:46035.

40. He M, Pan H, Chang RC, So KF, Brecha NC, Pu M. Activation of the Nrf2/HO-1 antioxidant pathway contributes to the protective effects of Lycium barbarum polysaccharides in the rodent retina after ischemia-reperfusion-induced damage. PLoS One 2014;9:e84800.

41. Bereczki D Jr, Balla J, Bereczki D. Heme oxygenase-1: clinical relevance in ischemic stroke. Curr Pharm Des 2018;24:2229-35.

42. Lu X, Gu R, Hu W, Sun Z, Wang G, Wang L, Xu Y. Upregulation of heme oxygenase-1 protected against brain damage induced by transient cerebral ischemia-reperfusion injury in rats. Exp Ther Med 2018;15:4629-36.

43. Taguchi K, Soma O, Tsuneishi S, Takada S, Nakamura H. Role of heme oxygenase-1 (HO-1) in hypoxic-ischemic insult of the newborn rat brain. Pediatr Res 1999;45:228.

44. Shah ZA, Nada SE, Doré S. Heme oxygenase 1, beneficial role in permanent ischemic stroke and in *Gingko biloba* (EGb 761) neuroprotection. Neuroscience 2011;180:248-55.

45. Kansanen E, Kuosmanen SM, Leinonen H, Levonen AL. The Keap1-Nrf2 pathway: Mechanisms of activation and dysregulation in cancer. Redox Biol 2013;1:45-9.

46. Loboda A, Damulewicz M, Pyza E, Jozkowicz A, Dulak J. Role of Nrf2/HO-1 system in development, oxidative stress response and diseases: an evolutionarily conserved mechanism. Cell Mol Life Sci 2016;73:3221-47.

47. Kensler TW, Wakabayashi N, Biswal S. Cell survival responses to environmental stresses via the Keap1-Nrf2-ARE pathway. Annu Rev Pharmacol Toxicol 2007;47:89-116.

48. Ye J, Piao H, Jiang J, Jin G, Zheng M, Yang J, Jin X, Sun T, Choi YH, Li L, Yan G. Polydatin inhibits mast cell-mediated allergic inflammation by targeting PI3K/Akt, MAPK, NF-κB and Nrf2/HO-1 pathways. Sci Rep 2017;7:11895.

49. Kaulmann A, Bohn T. Bioactivity of polyphenols: preventive and adjuvant strategies toward reducing inflammatory bowel diseases-promises, perspectives, and pitfalls. Oxid Med Cell Longev

2016;2016:9346470.

50. Scapagnini G, Vasto S, Abraham NG, Caruso C, Zella D, Fabio G. Modulation of Nrf2/ARE pathway by food polyphenols: a nutritional neuroprotective strategy for cognitive and neurodegenerative disorders. Mol Neurobiol 2011;44:192-201.

51. Ding Y, Zhang B, Zhou K, Chen M, Wang M, Jia Y, Song Y, Li Y, Wen A. Dietary ellagic acid improves oxidant-induced endothelial dysfunction and atherosclerosis: role of Nrf2 activation. Int J Cardiol 2014;175:508-14.

52. Badhani B, Sharma N, Kakkar R. Gallic acid: a versatile antioxidant with promising therapeutic and industrial applications. RSC Adv 2015;5:27540-57.

53. Kim SE, Lee MY, Lim SC, Hien TT, Kim JW, Ahn SG, Yoon JH, Kim SK, Choi HS, Kang KW. Role of Pin1 in neointima formation: down-regulation of Nrf2-dependent heme oxygenase-1 expression by Pin1. Free Radic Biol Med 2010;48:1644-53.